

A new approach to working coil design for a high frequency full bridge series resonant inverter fitted contactless induction heater

Sujit Dhar^{1a}, Biswajit Dutta^{2b}, Debasmita Ghoshroy^{3c}, Debabrata Roy^{*4}, Pradip Kumar Sadhu^{5d}, Ankur Ganguly^{4e}, Amar Nath Sanyal^{6f} and Soumya Das^{7g}

¹Department of Electrical and Electronics Engineering, Neotia Institute of Technology Management and Science, Jhinga, Diamond Harbour Road, South 24 Parganas, West Bengal 743368, India

²Department of Electrical Engineering, Seacom Engineering College, JL-2, Jaladhulagori, Sankrail, Howrah, West Bengal 711302, India

³Department of Electronics Engineering, Banasthali University, Niwai-Jodhpuriya Road, Vanasthali, Rajasthan 304022, India

⁴Department of Electrical Engineering, Techno India-Batanagar, B7-360/New, Ward No. 30, Maheshtala, West Bengal 700141, India

⁵Department of Electrical Engineering, Indian Institute of Technology (Indian School of Mines), Dhanbad, Jharkhand 826004, India

⁶Department of Electrical Engineering, Jadavpur University, Jadavpur, Kolkata, West Bengal 700032, India

⁷Department of Electrical Engineering, University Institute of Technology, Burdwan, West Bengal, India

(Received May 8, 2017, Revised August 27, 2017, Accepted September 2, 2017)

Abstract. High frequency full bridge series resonant inverters have become increasingly popular among power supply designers. One of the most important parameter for a High Frequency Full Bridge Series Resonant Inverter is optimal coil design. The optimal coil designing procedure is not a easy task.. This paper deals with the New Approach to Optimal Design Procedure for a Real-time High Frequency Full Bridge Series Resonant Inverter in Induction Heating Equipment devices. A new design to experimental modelling of the physical properties and a practical power input simulation process for the non-sinusoidal input waveform is accepted. The design sensitivity analysis with Levenberg-Marquardt technique is used for the optimal design process. The proposed technique is applied to an Induction Heating Equipment devices model and the result is verified by real-time experiment. The main advantages of this design technique is to achieve more accurate temperature control with a huge amount of power saving.

Keywords: induction heating; optimal design; COMSOL; full bridge inverter; resonant

*Corresponding author, Ph.D., E-mail: debabrataroy1985@gmail.com

^aAssistant Professor, E-mail: dhar.sujit@gmail.com

^bE-mail: biswajitdutta1985@gmail.com

^cE-mail: nupur1986.mtech@gmail.com

^dPh.D., E-mail: pradip_sadhu@yahoo.co.in

^ePh.D., E-mail: anksjc2002@yahoo.com

^fE-mail: ansanyal@yahoo.co.in

^gPh.D., E-mail: soumya.sd1984@gmail.com

Copyright © 2017 Techno-Press, Ltd.

<http://www.techno-press.org/?journal=acd&subpage=7>

ISSN: 2283-8477 (Print), 2466-0523 (Online)

1. Introduction

Due to high efficiency, precise control and low pollution properties, the induction heating is widely used not only in the industrial fields but also in the domestic appliances. In both cases, the need for the optimal design is increased to achieve more accurate temperature control for the compact packaging and the power saving demand at the present time (Kantar *et al.* 2016, Pitchai *et al.* 2016, Wang *et al.* 2014, Chakravorty *et al.* 2014). A lot of theoretical approaches have been reported. But, in the real applications, there are still some divergences between the theoretical and the real-time experimental results. The foremost whys and wherefores can be summarized as followings (Shin *et al.* 2016, Althaher *et al.* 2015, Kantar *et al.* 2015, Xu *et al.* 2015). Primarily, the physical thermal-parameters of the heating plates are not constant even in a physically linear range due to the structural disposition. When the usual axisymmetric coils are used, the parameters of the plates are varied due to the diameters and positions of the coils (Panigrahi *et al.* 2016). The values should be settled by the experimental modeling. Secondly in minor applications, such as domestic appliances, the devices should have a simple structure and should be compact (McKenna *et al.* 2015, Wang *et al.* 2014, Schweizer *et al.* 2013). To get a high frequency power for the induction heating from the 50 Hz home electric power, the high frequency full bridge series resonant inverter is commonly used, which produces an envelope waveform. It is quite different from the sinusoidal waveform, which is assumed in the theoretical analysis, both in the induced heat source amount and skin depth (Arteconi *et al.* 2013, Göttmann *et al.* 2013). The real-time design tool has to handle both properties. This paper describes an accurate optimal design procedure taking into account the experimental modeling and the practical power source simulation (Naar *et al.* 2013, Dev *et al.* 2013). The design sensitivity analysis with Levenberg-Marquardt method is adopted for the optimal design process. The proposed method is applied to the design of a Real-time High Frequency Full Bridge Series Resonant Inverter in Induction Heating Equipment devices (Pitchai *et al.* 2012, Richardson *et al.* 2010, Feng 2016).

2. Governing equations

The co-ordination to be solved is given by

$$j\omega\sigma(T)A + \nabla \times (\mu^{-1}\nabla \times A) = 0 \quad (1)$$

$$\rho C_p \frac{\partial T}{\partial t} - \nabla \cdot \kappa \nabla T = Q(T, A) \quad (2)$$

Where

ρ =Density

C_p =Specific Heat Capacity

κ =Thermal Conductivity

Q =Inductive Heating

The electric conductivity of copper σ is assumed by the expression

$$\sigma = \frac{1}{\left[\rho_0 (1 + \alpha (T - T_0)) \right]} \quad (3)$$

Where ρ_0 the resistivity at the reference temperature is $T_0=293K$, α is the temperature coefficient of the resistivity and T is the actual temperature in the domain.

The time average of the inductive heating over one period, is given by

$$Q = \frac{1}{2\sigma} |E|^2 \tag{4}$$

The coil inductor is cooled by a turbulent water flow in an internal cooling channel. This is matched by a combination of a high effective thermal conductivity and a homogenized out-of-plane convective loss term

$$Q_c = \frac{\frac{dM}{dt} C_\rho (T_{in} - T)}{2\pi r A} \tag{5}$$

Where

$\frac{dM}{dt}$ =The Water Mass Flow

T_{in} =The Water Inlet Temperature

r =The Radial Coordinate

A =The Cross Section Area of the Cooling Channel.

3. Orbital stability analysis of coil design system

Considered the system defined by the following equation

$$\begin{aligned} \dot{x}_1 &= x_1 g(r) - x_2 \\ \dot{x}_2 &= x_1 + x_2 g(r) \end{aligned} \tag{6}$$

Where $g(r) = r^2(A - r)$
 $r = \sqrt{x_1^2 + x_2^2}$

This system has a unique closed trajectory i.e., a limit cycle.

$$\begin{aligned} C: x^0(t) &= \begin{pmatrix} A \cos t \\ A \sin t \end{pmatrix} \\ x^0(t) &= x^0(t - 2\pi) \end{aligned} \tag{7}$$

It represents an oscillator stabilized at an amplitude $A > 0$; and its equation of first variation about $x^0(t)$ are

$$\begin{pmatrix} y_1 \\ y_2 \end{pmatrix} = \begin{pmatrix} -A^3 \cos^2 t & (-1 - A^3 \sin t \cos t) \\ (1 - A^3 \sin t \cos t) & -A^3 \sin^2 t \end{pmatrix} \begin{pmatrix} y_1 \\ y_2 \end{pmatrix} \tag{8}$$

It can be verified by substitution into Eq. (8) that a fundamental matrix for this system is

$$\phi(t) = \begin{pmatrix} \cos t & -\sin t \\ \sin t & \cos t \end{pmatrix} \begin{pmatrix} \varepsilon^{-A^3 t} & 0 \\ 0 & 1 \end{pmatrix} \quad (9)$$

The characteristic multipliers

$$\begin{aligned} \lambda_1 &= \varepsilon^{-2\pi A^3} \\ \lambda_2 &= 1 \end{aligned} \quad (10)$$

As expected one multiplier is on the unit cycle. The above equation satisfies the orbital stability theorem. So the Coil Design system is stable.

4. Conservation of energy in coil design system

Consider the system shown in Fig. 2 consisting of two parallel current-carrying conductors of length l . One is fixed and the other is constrained by springs with total spring constant k . Neglecting firing effects, equation can be written with the total force f on the movable conductor as.

$$f(x) = -kx + \frac{\mu_0 l i^2}{2\pi(d-x)} \quad (11)$$

μ_0 = Permeability of free space
According to following equation

$$\frac{\rho d\rho}{m} = f(x) dx \quad (12)$$

Becomes

$$\frac{\rho d\rho}{m} = \left[-kx + \frac{\mu_0 l i^2}{2\pi(d-x)} \right] dx \quad (13)$$

And can be integrated to yield

$$\frac{\rho^2}{2m} + \frac{1}{2} kx^2 + \frac{\mu_0 l i^2}{2\pi} \ln(d-x) = h \quad (14)$$

Which is the total energy in the system.

The term $\frac{\rho^2}{2m}$ can be identified as the kinetic energy and the remaining terms on the left-hand side of equation 14 comprises of the potential energy $\mu(x)$ stored in the force field. This is actually a combination of energies stored in the spring and the magnetic field.

5. Error analysis in energy conservation using FEM

$$-\frac{d^2u}{dx^2} = 2 \quad \text{for } 0 < x < 1 \quad (15)$$

With $\mu(0)=\mu(1)=0$
The exact solution is

$$\mu(x) = \mu(1-x) \quad (16)$$

While the finite element solutions are for $N = 2$

$$\mu_h = \begin{cases} h^2 \left(\frac{x}{h} \right) & \text{for } 0 \leq x \leq h \\ h^2 \left(2 - \frac{x}{h} \right) & \text{for } h \leq x \leq 2h \end{cases} \quad (17)$$

$N = 3$

$$\mu_h = \begin{cases} 2h^2 \left(\frac{x}{h} \right) & \text{for } 0 \leq x \leq h \\ 2h^2 \left(2 - \frac{x}{h} \right) + 2h^2 \left(\frac{x}{h} - 1 \right) & \text{for } h \leq x \leq 2h \\ 2h^2 \left(3 - \frac{x}{h} \right) & \text{for } 2h \leq x \leq 3h \end{cases} \quad (18)$$

$N = 4$

$$\mu_h = \begin{cases} 3h^2 \left(\frac{x}{h} \right) & \text{for } 0 \leq x \leq h \\ 3h^2 \left(2 - \frac{x}{h} \right) + 4h^2 \left(\frac{x}{h} - 1 \right) & \text{for } h \leq x \leq 2h \\ 4h^2 \left(4 - \frac{x}{h} \right) + 3h^2 \left(\frac{x}{h} - 2 \right) & \text{for } 2h \leq x \leq 3h \\ 3h^2 \left(4 - \frac{x}{h} \right) & \text{for } 3h \leq x \leq 4h \end{cases} \quad (19)$$

For the two-element case $h = 0.5$, the errors are given by

$$\begin{aligned} \|\mu - \mu_h\|_0^2 &= \int_0^h (x - x^2 - hx)^2 dx + \int_h^1 (x - x^2 - 2h^2 + hx)^2 dx = 0.002083 \\ \left\| \frac{d\mu}{dx} - \frac{d\mu_h}{dx} \right\|_0^2 &= \int_0^h (1 - 2x - h^2)^2 dx + \int_h^1 (1 - 2x + h^2)^2 dx = 0.08333 \end{aligned} \quad (20)$$

Table 1 Error in the energy conservation

h	$\log_{10} h$	$\ e\ _0$	$\log_{10} \ e\ _0$	$\ e\ _1$	$\log_{10} \ e\ _1$
$\frac{1}{2}$	-0.301	0.04564	-1.341	0.2887	-0.5396
$\frac{1}{3}$	-0.477	0.02028	-1.693	0.1925	-0.7157
$\frac{1}{4}$	-0.601	0.01141	-1.943	0.1443	-0.8406

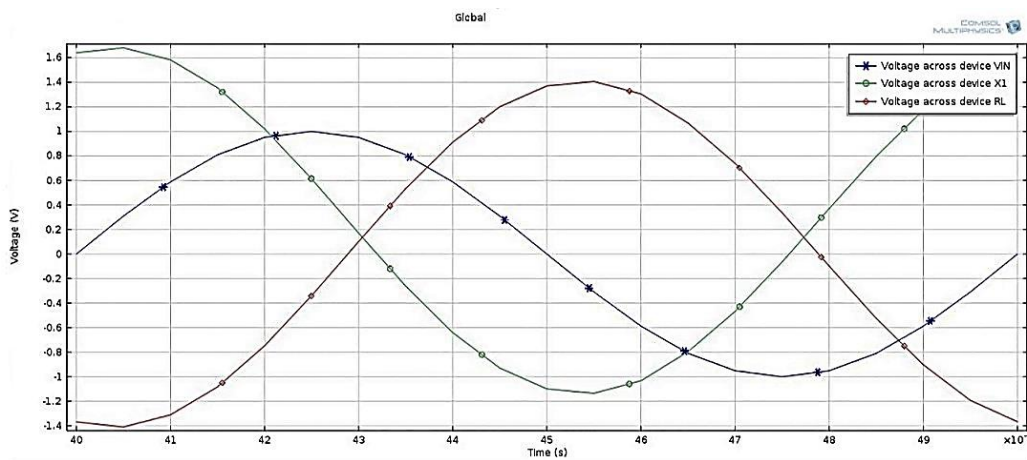


Fig. 1 The approximated shape

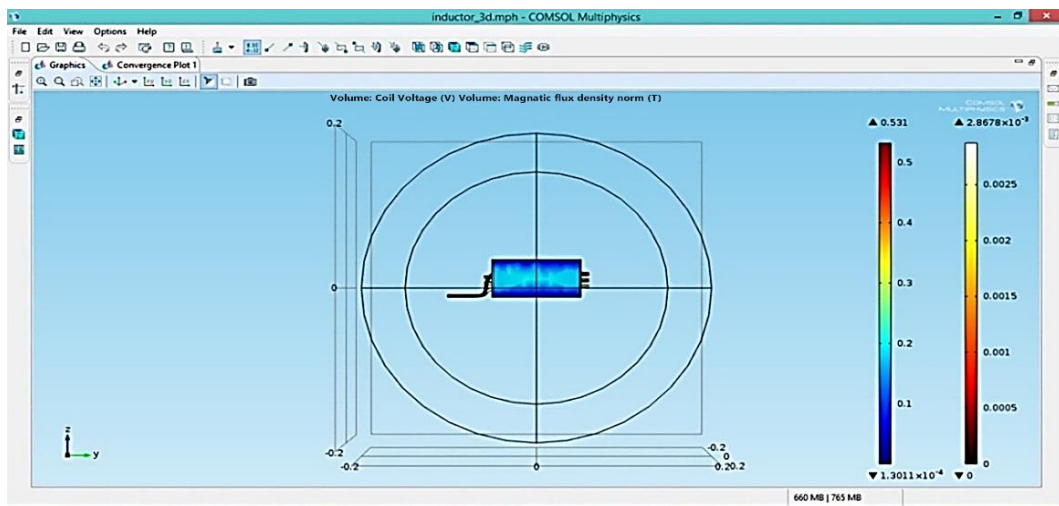


Fig. 2 The shape of the induction heating equipment devices

Similar calculations can be performed for $N = 3$ and $N = 4$ Following Table gives the errors for $N = 2, 3, 4$.

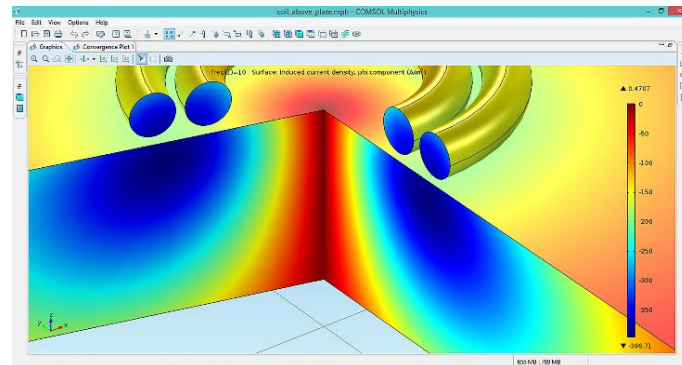


Fig. 3 The design parameters in the optimal design process(3D)

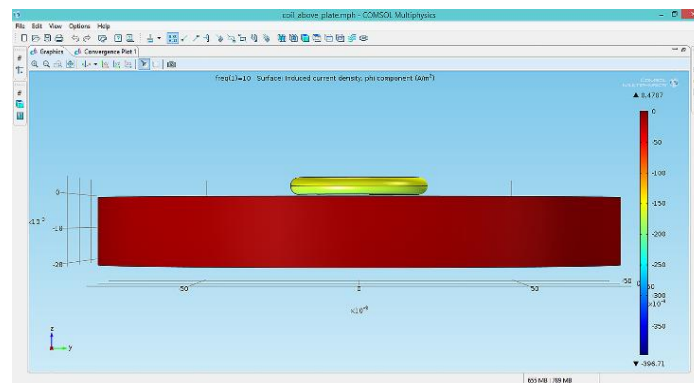


Fig. 4 The design parameters in the optimal design process (2D)

Table 2 Error in the energy conservation

Description	Expression
Supply Voltage	240 V
Wire Conductivity	5483.165792 S/n
Wire Radius in Coil	0.05 mm
Frequency	55 Khz
Turns in coil	40
Time for Stationary Solution	1 sec

6. The practical power input simulation results and analysis

In the real-time analysis of the eddy current system the input current was time harmonic sinusoidal wave but the actual power input of the cooker is an envelope waveform as shown in Fig. 1.

7. Optimal design procedure for a real-time high frequency full bridge series resonant inverter in induction heating equipment devices

The Optimal Design model for a Real-time High Frequency Full Bridge Series Resonant Inverter in Induction Heating equipment devices is shown in Fig. 2. The design parameters of the induction heating equipment devices considered here are the width and location of the gap between exciting coils mainly is shown in Fig. 3. The size of the central hole and the end diameter are fixed in the design. The design parameters in the optimal design process is shown in Fig. 4. Table 1 give the results of error in the Conservation of Energy in the coil Design System and Table 2 give the error in the Optimal Design Procedure for a Real-Time High Frequency Full Bridge Series Resonant Inverter in Induction Heating Equipment Devices and Fig. 4 shown the design parameters in the optimal design process (2D).

8. Conclusions

An optimal design procedure for a Real-Time High Frequency Full Bridge Series Resonant Inverter in Induction Heating Equipment device is proposed. Temperature distribution of the pan after optimization is modelled through an experiment. Also, non-sinusoidal exciting current is taken into account by the inverter simulation program and the actual power input waveform of the induction cooker is to be considered. The temperature distribution of the system is computed by finite element method and compared with experimental determinations. The Levenberg-Marquardt technique is used for the optimal design with real-time limitations. The new experimental and simulation data are similar, proving the validity of the proposed technique.

References

- Althaher, S., Mancarella, P. and Mutale, J. (2015), "Automated demand response from home energy management system under dynamic pricing and power and comfort constraints", *IEEE Trans. Smart Grid.*, **6**(4), 1874-1883.
- Arteconi, A., Hewitt, N.J. and Polonara, F. (2013), "Domestic demand-side management (DSM): Role of heat pumps and thermal energy storage (TES) systems", *Appl. Therm. Energy*, **51**(1), 155-165.
- Chakravorty, D., Chaudhuri, B. and Hui, S.Y.R. (2016), "Rapid frequency response from smart loads in Great Britain power system", *IEEE Trans. Smart Grid.*, **PP**(99), 1.
- Dev, S.R.S., Gariépy, Y., Orsat, V. and Raghavan, G.S.V. (2012), "Finite element modeling for optimization of microwave heating of in-shell eggs and experimental validation", *J. Numer. Modell. Electron. Netw., Dev. Field.*, **25**(3), 275-287.
- Feng, F. (2016), "3D finite element analysis of the whole-building behavior of tall building in fire", *Adv. Comput. Des.*, **1**(4), 329-344.
- Göttmann, A., Bailly, D., Bergweiler, G., Bambach, M., Stollenwerk, J. and Hirt, G. (2013), "A novel approach for temperature control in SPIF supported by laser and resistance heating", *J. Adv. Manuf. Technol.*, **67**(9), 2195-2205.
- Kantar, E. and Hava, A.M. (2016), "Optimal design of grid-connected voltage-source converters considering cost and operating factors", *IEEE Trans. Ind. Electron.*, **63**(9), 5336-5347.
- Karmaker, H., Ho, M. and Kulkarni, D. (2015), "Comparison between different design topologies for multi-megawatt direct drive wind generators using improved second generation high temperature superconductors", *IEEE Trans. Appl. Supercond.*, **25**(3), 1-5.
- McKenna, K. and Keane, A. (2015), "Residential load modeling of price-based demand response for network impact studies", *IEEE Trans. Smart Grid.*, **7**(5), 1-10.
- Naar, R. and Bay, F. (2013), "Numerical optimization for induction heat treatment processes", *Appl. Math.*

- Model.*, **37**(4), 2074-2085.
- Panigrahi, S.K. and Das, K. (2016), "Ballistic impact analyses of triangular corrugated plates filled with foam core", *Adv. Comput. Des.*, **1**(2), 139-154.
- Pitchai, K., Birla, S.L., Jones, D. and Subbiah, J. (2012), "Assessment of heating rate and non-uniform heating in domestic microwave ovens", *J. Microw. Pow. Electromagn. Energy*, **46**(4), 229-240.
- Pitchai, K., Chen, J., Birla, S., Jones, D. and Subbiah, J. (2016), "Modeling microwave heating of frozen mashed potato in a domestic oven incorporating electromagnetic frequency spectrum", *J. Food Eng.*, **173**(1), 124-131.
- Richardson, I., Thomson, M., Infield, D. and Clifford, C. (2010), "Domestic electricity use: A high-resolution energy demand model", *Energy Build.*, **42**(10), 1878-1887.
- Schweizer, M. and Kolar, J.W. (2013), "Design and implementation of a highly efficient three-level T-type converter for low-voltage applications", *IEEE Trans. Pow. Electron.*, **28**(2), 899-907.
- Schweizer, M., Friedli, T. and Kolar, J. (2013), "Comparative evaluation of advanced three-phase three-level inverter/converter topologies against two-level systems", *IEEE Trans. Ind. Electron.*, **60**(12), 5515-5527.
- Shin, D., Lee, J.P., Yoo, D.W. and Kim, H.J. (2015), "Stability improvement of interleaved voltage source inverters employing coupled inductors for grid-connected applications", *IEEE Trans. Ind. Electron.*, **62**(10), 6014-6023.
- Wang, Z., Shi, X., Tolbert, L. and Wang, F. (2016), "Temperature-dependent short-circuit capability of silicon carbide power MOSFETs", *IEEE Trans. Pow. Electron.*, **31**(2), 1555-1566.
- Wang, Z., Shi, X., Xue, Y., Tolbert, L., Wang, F. and Blalock, B. (2014), "Design and performance evaluation of overcurrent protection schemes for silicon carbide power MOSFETs", *IEEE Trans. Ind. Electron.*, **61**(10), 5570-5581.
- Xu, Y. and Milanovic, J.V. (2015), "Artificial-intelligence-based methodology for load disaggregation at bulk supply point", *IEEE Trans. Pow. Syst.*, **30**(2), 795-803.